Optimized polybutylene terephthalate powders for selective laser beam melting

Jochen Schmidt[a, b*], Marius Sachs[a, b], Stephanie Fanselow[a, b], Meng Zhao[c], Stefan Romeis[a, b], Dietmar Drummer[b, c], Karl-Ernst Wirth[a, b] and Wolfgang Peukert[a, b]

[a] Institute of Particle Technology, Friedrich-Alexander-Universität Erlangen-Nürnberg, Cauerstraße 4, D-91058 Erlangen, Germany
[b] Interdisciplinary Center for Functional Particle Systems, Friedrich-Alexander-Universität Erlangen-Nürnberg, Haberstraße 9a, D-91058 Erlangen, Germany
[c] Institute of Polymer Technology, Friedrich-Alexander-Universität Erlangen-Nürnberg, Am Weichselgarten 9, D-91058 Erlangen, Germany

Authors email addresses:
jochen.schmidt@fau.de (J. Schmidt), marius.sachs@fau.de (M. Sachs), stephanie.fanselow@fau.de (S. Fanselow), zhao@lkt.uni-erlangen.de (M. Zhao), stefan.romeis@fau.de (S. Romeis), drummer@lkt.uni-erlangen.de (D. Drummer), karl-ernst.wirth@fau.de (K.-E. Wirth), wolfgang.peukert@fau.de (W. Peukert)

* Corresponding author:
Dr. Jochen Schmidt
Tel. +49 9131 8529408
Fax: +49 9131 8529402
Email: jochen.schmidt@fau.de

Publisher's version:
Chemical Engineering Science 156 (2016) 1–10
https://doi.org/10.1016/j.ces.2016.09.009

Graphical Abstract

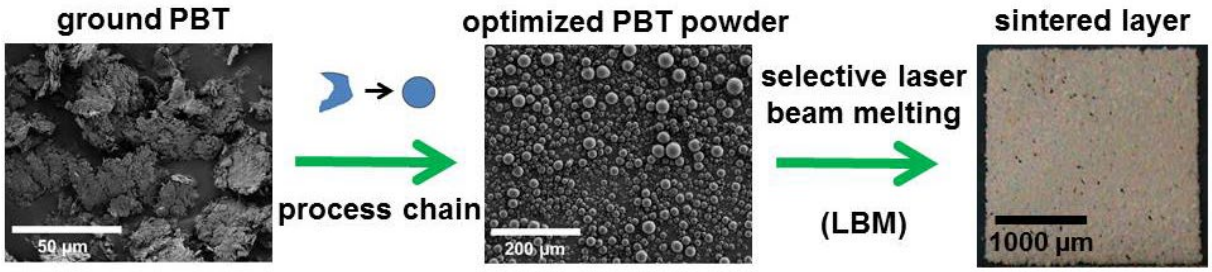

Highlights

- process chain for producing polybutylene terephthalate (PBT) powders for selective laser beam melting (LBM)
- processability of powders is assessed by characterization of sintered thin layers
- influence of particle shape and size on processability in LBM is studied
- good LBM processability is observed for PBT powders of good flowability
- device quality is remarkably influenced by powder flowability and bulk density

Keywords

poly butylene terephthalate
wet grinding
downer reactor
dry particle coating
flowability
selective laser beam melting

Abstract

Additive manufacturing processes like selective laser beam melting of polymers (LBM) are established for production of prototypes and individualized parts. The transfer to serial production currently is hindered by the limited availability of polymer powders with good processability.

Within this contribution the effect of powder properties, such as particle size, shape and flowability on the processability in LBM and their influence on device quality is exemplified for polybutylene terephthalate (PBT) materials. A process chain for the production of spherical polymer microparticles has been developed to obtain PBT powder materials. The process chain consists of three steps: First, polymer microparticles are produced by wet grinding. Second, the particle shape is engineered by rounding in a heated downer reactor to improve the flowability of the product. A further improvement of flowability of the still cohesive spherical PBT particles is realized by dry coating with fumed silica.

Moreover, properties of the PBT powders obtained along the process chain are thoroughly characterized with respect to structure and crystallinity by infrared spectroscopy, X-ray diffraction and differential scanning calorimetry. The effect of flowability, shape and bulk density on the powders' processabilities in LBM is assessed by characterization of the quality of thin layers built in a LBM device. It is demonstrated that the device quality is strongly determined by particle properties: powders of good flowability and high bulk density are mandatory to obtain dense devices.

1. Introduction

Additive manufacturing methods allow the tool-free and formless production of complex structures. Especially selective laser beam melting (LBM) of polymers as a generative powder- and beam-based manufacturing process is promising. Several years ago, generative manufacturing methods almost exclusively have been applied in the production of parts at low piece numbers in applications where mechanical properties of the built devices typically were of minor importance (rapid prototyping). With the advent of additive manufacturing, i.e. the application of generative methods in mass production – commonly referred to as '3D printing'- new requirements with respect to process stability and robustness, mechanical properties of the devices, as well as new demands concerning the powder materials used in beam- and powder-based additive manufacturing methods have been defined (Kruth et al., 2003; Wendel et al., 2008; Drummer et al., 2010; Goodridge et al., 2012; Schmidt et al., 2014; Wohlers, 2014; Schmid, 2015; Witt, 2016). Preferentially semi-crystalline thermoplasts are applied in the manufacture of functional components via LBM because of their improved mechanical properties as compared to amorphous polymers (Wohlers, 2014; Schmid, 2015). Currently, the spectrum of commercially available LBM powder materials is very limited, about 95 % of the total market share is made up of polyamide (PA) - based materials. PA powders are typically produced by bottom-up approaches (c.f. emulsion polymerization) or precipitation processes are applied (Wohlers, 2014; Schmid, 2015). Besides PA, polystyrene and polypropylene as well as thermoplastic elastomers or PEEK are available (Goodridge et al., 2012; Wohlers, 2014). In addition to the aforementioned bottom-up processes, also top-down approaches like cryogenic (dry) grinding (Wilczek et al., 2004; Bertling and Eloo, 2009), wet grinding of polymers (Schmidt et al., 2012), co-extrusion (Schmid, 2015) or melt emulsification (Fanselow et al., 2016) have been proposed to produce polymer microparticles.

To further extend the applications of LBM new and cheap materials with good processability must be supplied: device quality, LBM processability and powder properties (Blümel et al., 2015; Ziegelmeier et al., 2015) are directly connected. Moreover, innovative and versatile processes being applicable to a wide variety of thermoplasts are desirable.

Wet grinding as a top-down approach is established for the production of micro- and even nanoparticles for a variety of materials (Damm et al., 2013; Romeis et al., 2014; Nacken et al., 2015; Ito et al., 2016). However, typically irregular-shaped, cohesive particles are obtained that cannot be employed in LBM without further modification. Therefore, a process route for production of spherical polymer microparticles with good flowability consisting of wet grinding (Schmidt et al., 2012; Wolff et al., 2014; Schäfer et al., 2016), rounding of the irregular-shaped comminution product in a heated downer reactor and a dry coating step (Pfeffer et al., 2001; Yang et al., 2005; Blümel et al., 2015) has been proposed and successfully applied to polystyrene (Schmidt et al., 2014). Compared to dry grinding, wet grinding of polymers allows for much smaller product particles giving the opportunity to lower the size range of LBM materials. If appropriate process conditions, i.e. low-viscous solvents and a moderately reduced process temperature are chosen, particles smaller than 10 microns ($x_{50,3}$) are readily obtained for a variety of engineering and high performance plastics. For brittle, amorphous polymers like polystyrene even smaller product particles ($x_{50,3}$ < 2 µm) can be produced (Schmidt et al., 2012). LBM materials of small particle size are desirable because they allow for higher surface qualities (lower surface roughness) of the obtained parts and better resolution (Kruth et al., 2003). However, the commercially available polymer powders for additive manufacturing are so far in the size range of 50 to 70 microns ($x_{50,3}$) due to concerns regarding the processability: with smaller particles inhomogeneous coating during powder deposition in LBM due to poor flowability may occur. We demonstrate that these problems can be overcome by rounding the irregular shaped comminution product and dry coating (Pfeffer et al., 2001) of the obtained spherical particles. By dry coating the surface roughness is increased on the nanoscale leading to an overall decrease of interparticulate van der Waals forces (Rumpf, 1974; Zhou et al., 2003; Götzinger and Peukert, 2004; Linsenbühler and Wirth, 2005; Zhou and Peukert, 2008).

Within this contribution the process chain is applied to produce spherical polybutylene terephthalate (PBT) powders of good flowability and processability. To our knowledge at present optimized PBT powders are not available for laser beam melting of polymers. However, this semi-crystalline thermoplastic shows good mechanical properties (e.g. impact resistance) and, thus, is of potential interest for LBM in a variety of applications, e.g. in the automotive industries. The PBT product particles are thoroughly characterized with respect to both, powder properties and polymer structure: Powder flowability is assessed by means of tensile strength measurements. Differential scanning calorimetry (DSC), infrared (IR) spectroscopy and X-ray diffraction (XRD) are applied to monitor the structural evolution of the polymer along the process chain. An improvement of flowability by a factor of about 5 is achieved by subsequent rounding of the comminution product and dry coating as proven by tensile strength measurements of the powders. Moreover, only minor changes in crystallinity

of the semi-crystalline polymer have been observed, which is of importance for the mechanical properties of components built via LBM. The processability (Gibson and Shi, 1997) of the obtained powders is demonstrated by building thin layer specimens. The thin layers demonstrate that the device quality is directly affected by powder properties. Especially flowability is crucial: powders that show good flowability and high bulk density are the prerequisite to obtain dense parts via LBM (Blümel et al., 2015).

2. Materials and methods

2.1 Materials

As raw material PBT 4520 Ultradur Highspeed (BASF) of a density of 1.30 g/cm^3, as determined by helium pycnometry, has been applied. The raw PBT material has been supplied as granules with size between 2 mm and 3 mm. The following PBT powders have been characterized and evaluated with respect to their LBM processability:

- A micro particulate PBT powder consisting of irregular, plate-like PBT microparticles referred to as ’ground PBT’ was produced by wet comminution.
- Rounded PBT microparticles referred to as ’rounded PBT’ were obtained by rounding ground PBT using a heated downer reactor.
- Finally, PBT microparticles of improved flowability referred to as ‘rounded & dry coated PBT’ were produced by dry coating of rounded PBT powder with fumed silica.

The processes applied to obtain the aforementioned powders and the powder characteristics are outlined in detail in the experimental and the results section (sections 2.3 and 2.4).
Denatured ethanol (95 %, VWR) has been used as solvent in wet grinding. Fumed silica (Evonik Industries) with a primary particle size of about 7 nm has been applied for dry coating of rounded PBT powders.

2.2 Characterization methods

2.2.1 Laser diffraction particle sizing

Particle size distributions of the produced powders were determined by laser diffraction particle sizing using a Mastersizer 2000 / Hydro 2000S (Malvern). In the case of wet grinding, the ethanolic product suspensions have been diluted as appropriate prior to measurement in the dispersing unit using an aqueous sodium dodecyl sulphate solution (SDS, 98% (Merck)) to ensure dispersion stability. Dry samples after size reduction or rounding have been dispersed in aqueous SDS solution as well. Prior to particle sizing ultrasonication of the dispersions has been performed.

2.2.2 Scanning Electron Microscopy

The polymer particles have been characterized by scanning electron microscopy (SEM) using a Gemini Ultra 55 (Zeiss) device equipped with a through-the-hole detector. An acceleration voltage of 1 kV has been applied. SEM images were taken at appropriate magnifications.

2.2.3 Powder flowability

Flowability of the products was assessed using a tensile strength tester (Schweiger and Zimmermann, 1999; Meyer and Zimmermann, 2004). A load of 153 Pa was applied to the powders. For details on the measurement procedure, see (Schmidt et al., 2014).

2.2.4 Infrared spectroscopy

Infrared (IR) spectra were recorded in transmission in the spectral range from 4000 cm^{-1} to 400 cm^{-1} at a resolution of 2 cm^{-1} using a FT-IR spectrometer FTS 3100 (Varian). The polymer powder samples were dispersed in KBr (UVASol, Merck) at appropriate concentration (ratio of about 1:100 (mass polymer / mass KBr)) and platelets were produced. Reported spectra are normalized to their respective maximum absorbance; baseline corrections were performed manually.

2.2.5 Differential Scanning Calorimetry

Characterization by differential scanning calorimetry (DSC) was performed at a heating rate of 20 K min^{-1} using a DSC8000 (Perkin Elmer).

2.2.6 X-ray diffraction

Structural analysis of the polymers by means of powder X-ray diffraction (XRD) was performed using a Bruker AXS D8 Advance diffractometer. The device was equipped with a VANTEC-1 detector and a Ni filter. Cu K_α radiation (λ = 154.06 pm) was used. The X-ray patterns were recorded in Bragg-Brentano geometry in the range $10° \leq 2\theta \leq 60°$. The step width was 0.014° and the accumulation time was 1 s for each step.

2.2.7 He pycnometry

Density was determined using the Helium pycnometer AccuPyc 1330 (Micromeritics). Reported values for densities are the average from three independent determinations.

2.2.8 Image analysis / Quantification of powder deposition

To assess the powder deposition behavior of the different PBT powders doctor blading was applied. A Quadruple Film Applicator Model 360 (Erichsen) was used. The gap size was 120

µm. A black-colored paper was used as substrate to allow for the quantification of the area covered with powder using the commercial program “Image J” for image analysis. The coverage of the substrate with powder determined by this model experiment allows to assess the processability of the material in the LBM process during the deposition step (for details see (Blümel et al., 2015)).

2.2.8 Profilometry

To characterize the quality of thin layers built via selective laser beam melting of polymers in terms of the layers’ root mean square (rms) roughness, a tactile profilometer DektakXT (Bruker) was applied. The scan speed was 100 µm/s, the horizontal resolution was 333 nm and the vertical resolution 8 nm.

2.3 Experimental setup

2.3.1 Comminution (dry grinding)

A coarse PBT powder of size $x_{50,3}$ = 239 µm (‘PBT < 0.5 mm’) has been obtained using a rotary impact mill Pulverisette-14 (Fritsch) operated at 20000 min^{-1}. The mill was equipped with a pin rotor and a sieve ring of 0.5 mm mesh size. The PBT feed has been pre-cooled using liquid nitrogen prior to impact comminution. The impact-comminuted PBT has been used as feed material for wet grinding. The particle size distribution (volume sum, Q_3) of the sample PBT < 0.5 mm as obtained by laser diffraction particle sizing is given in Figure 1. PBT < 0.5 mm exhibits a quite narrow distribution with a $x_{10,3}$ of 79 µm and a $x_{90,3}$ of 550 µm (span ($x_{90,3}$ - $x_{10,3}$) / $x_{50,3}$ = 1.97).

2.3.2 Comminution (wet grinding)

Wet grinding experiments have been performed using a batch stirred media mill PE5 (Netzsch) equipped with a three-disc stirrer. The stirrer discs are made of polyethylene and the volume chamber of the stirred media mill is lined with silicon nitride ceramics. A mass fraction of about 18.5 % of PBT feed material ‘PBT < 0.5 mm’ has been used and denatured ethanol was used as solvent. A stress energy SE (see equation 1) (Kwade, 1999) of 1.91 mJ was selected by setting the stirrer tip speed v_{tip} (circumferential speed of the discs) to 6.3 m s^{-1} (equaling 800 min^{-1}) and using Yttria-stabilized ZrO_2 grinding beads (YSZ, Tosoh) of diameter d_{GM} = 2.0 mm and a density of ρ_{GM} = 6050 kg m^{-3}. The maximum energy that may be transferred to a product particle by the collision of two grinding beads SE_{max} is proportional to the kinetic energy of the grinding media.

(eq. 1) $$SE_{max} \propto \rho_{GM} \cdot d_{GM}^3 \cdot v_{tip}^2$$

Approximately 14.3 kg of grinding media were filled into the grinding chamber. The process temperature has been adjusted to (20 +/- 2) °C using cooling water. The particle size

distribution (volume sum, Q_3) of ground PBT obtained after a process time of 345 minutes is depicted in Figure 1. The wet ground polymer shows a rather broad size distribution with $x_{50,3}$ = 25.2 µm ($x_{10,3}$ = 6.6 µm, $x_{90,3}$ = 275.5 µm, span= 10.67). Prior to rounding the cohesive PBT microparticles were separated from the product suspension by centrifugation and dried at 100°C.

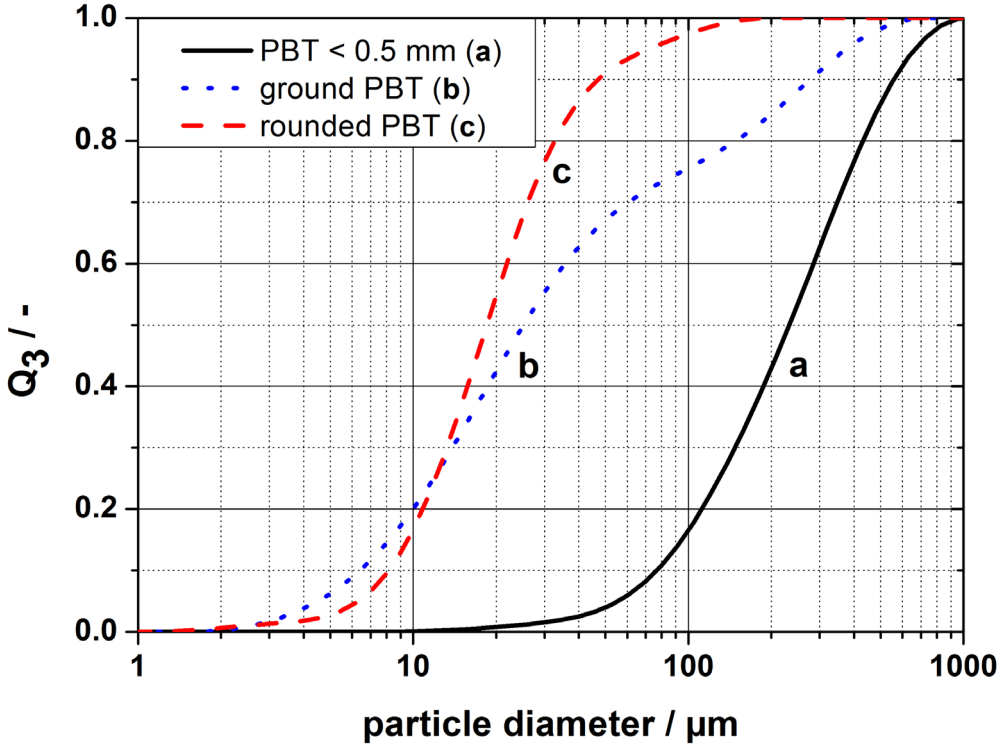

Figure 1: Particle size distributions (volume sum, Q_3) of PBT powders obtained by cryogenic grinding in a rotor impact mill (PBT < 0.5 mm), wet grinding (ground PBT) and after rounding in a downer reactor (rounded PBT).

2.3.3 Rounding (downer reactor)

The rounding was performed in a heated downer reactor made of stainless steel with a diameter of 100 mm and a heated length of 4.5 m where the particles are molten, rounded and solidified, respectively. The heating is achieved using a nine stage heating system (Thermal Technology). As inert carrier gas nitrogen (purity 5.0, Linde Gas) is used to minimize aging effects of the polymer like e.g. oxidative degradation. Powder dispersion is achieved by using a PALAS RGB 1000 powder disperser. The shear forces applied by this dispersion unit are sufficient for the dispersion of the polymer particles within the aerosol (Niedballa, 1999). In order to minimize contact of the molten polymer particles and the hot reactor walls, a special aerosol inlet was developed: The aerosol enters the downer in the center of the reactor's cross section. A sheath gas flow (nitrogen) is applied and surrounds the aerosol in order to minimize the contact of polymer particles and reactor wall. To achieve

a homogenous distribution of the sheath gas, this flow passes a sintered metal plate. Further details on the reactor setup as well as the rounding process and the selection of proper process parameters can be found elsewhere (Schmidt et al., 2014). A scheme of the setup is shown in Figure 2.

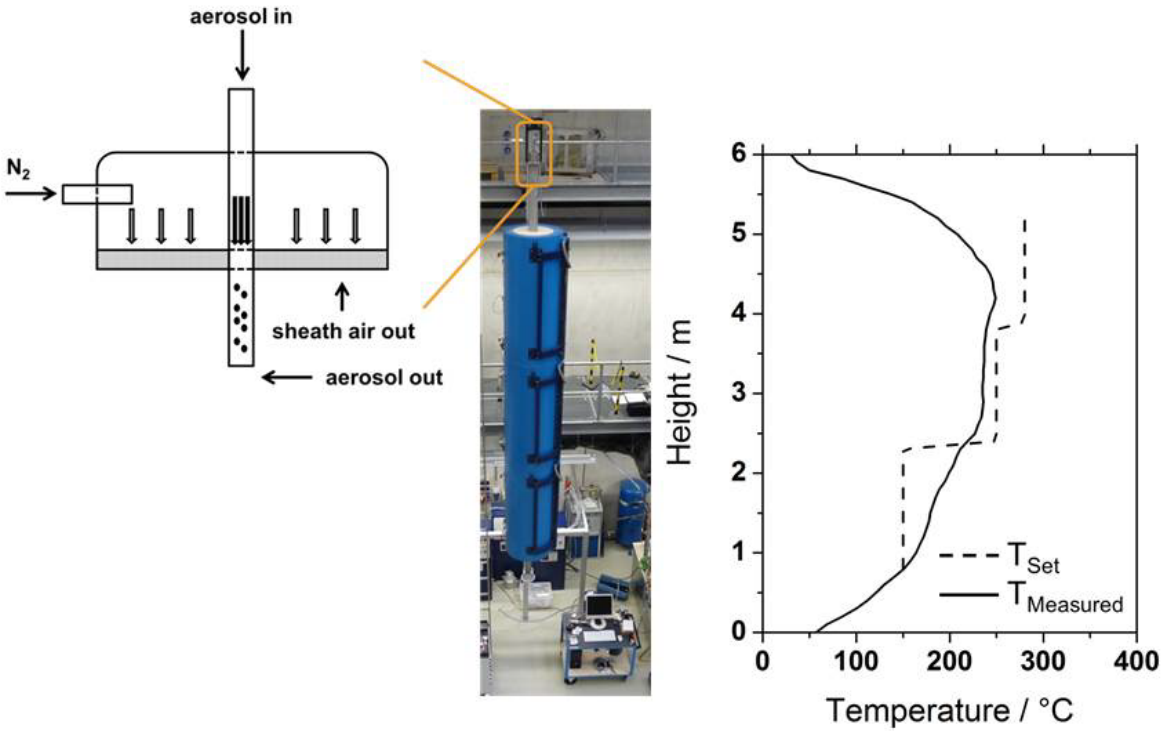

Figure 2: Detail of the aerosol inlet (left) and photograph (middle) of the heated downer reactor used for rounding of polymer particles; right: gas temperature ($T_{Measured}$) in the downer reactor over the reactor height vs. set temperature T_{Set} (heating system).

The temperature profile along the reactor height depicted in Figure 2 (right) was measured in the center of the reactor cross section under inert gas flow (7 m^3/h) using thermocouples. For comparison the set temperature T_{Set} of the oven system is shown as well. The slight difference between the set temperature T_{Set} and the measured temperature $T_{Measured}$ is due to heat transfer along the reactor cross section, heat transfer along the reactor height (in z direction) and heating up of the inert gas flow. The reactor can be divided into different zones with respect to process temperature. In the first zone (height = 5.5 m … 4 m) the overall gas flow is gradually heated to a process temperature above 230 °C necessary for rounding of PBT. The time necessary to heat the core of the polymer microparticles to the gas temperature is in the range of several milliseconds and, thus, can be neglected (Schmidt et al., 2014). The heat exchange is mainly due to convective and conductive heat transfer from the surrounding gas to the particles. Due to the small size of the polymer particles and the

rather low temperatures heat exchange due to radiation can be neglected (Kirchhof et al., 2009). In the second zone (height = 4 m … 2.5 m), the constant process temperature above the melting temperature of the polymer is maintained to complete the rounding. In the third zone (height = 2.5 m … 1 m) the consolidation of the polymer melt takes place and solidification occurs. To avoid unwanted thermodiffusion effects, the temperature is gradually reduced to about 150 °C. In the unheated zone (height = 1 m … 0 m) further cooling of the aerosol close to room temperature is accomplished. The solid particles are separated at the bottom of the reactor from the carrier gas using a sintered metal plate (GKN Sinter Metals). The particle size distribution (volume sum, Q_3) of rounded PBT obtained is given in Figure 1. During the rounding process obviously some of the coarse particles get lost either due to e.g. improper aerosol generation or due to adhesion onto reactor components and successive decomposition of the polymer. The total yield of rounded product expressed as the mass ratio of feed particles and product particles recovered typically is around 75 %.

2.3.4 Dry particle coating

Dry particle coating was performed using a tumbling mixer (T2F, Willy A. Bachofen AG). The polymer host particles were mixed at 72 min^{-1} in 1200 ml aluminum bottles for 10 minutes with fumed silica guest particles. A mass concentration of 0.1 % of silica with respect to polymer has been applied. For details on dry coating of polymers and its influence on flowability e.g. refer to previous work (Schmidt et al., 2014; Blümel et al., 2015).

2.3.5 Laser beam melting of PBT powders

To assess the LBM processability thin layer specimens of 24 mm * 24 mm size (Drexler et al., 2013; Drummer et al., 2015) have been built using a Sinterstation 2000 (DTM) laser sintering machine. The building temperature was 210 °C. The device is equipped with a CO_2 laser source. A nominal laser power of P_L = 2.5 W (laser focus diameter d_f = 0.4 mm) and a scan speed of v_s = 0.333 m/s have been applied. The hatch distance was 0.25 mm. The energy input with respect to laser beam area E_{beam} was 23.9 mJ/mm^2 and may be calculated according to equation 2:

$$\text{(eq. 2)}\quad E_{beam} = \frac{4 \cdot \pi \cdot P_L}{d_f \cdot v_s}$$

3. Results and Discussion

3.1 Wet grinding of polybutylene terephthalate

With respect to finer product particles wet grinding of polymers (Schmidt et al., 2012; Wolff et al., 2014) has been shown to be advantageous as compared to alternative top-down approaches typically used for comminution of plastic or visco-elastic materials applying cutting mills, rotor impact mills or jet mills (Landwehr and Pahl, 1986; Wilczek et al., 2004; Juhnke and Weichert, 2005; Weber et al., 2006; Bertling and Eloo, 2009). Figure 3a depicts the evolution of the particle sizes $x_{10,3}$, $x_{50,3}$ and $x_{90,3}$ over process time. During the first 100 to 120 minutes of wet grinding only slight size reduction is observed. A similar behavior has been previously reported for wet grinding of PEEK (Schmidt et al., 2012) and has also been observed for polyethylene terephthalate. Although these grinding kinetics are uncommon in wet grinding of (brittle) inorganic substances, they seem to apply to non-brittle polymers showing large breakage elongation and fracture toughness. In the later course of processing a continuous reduction of product particle size occurs. The particle size distribution first broadens: typically bimodal particle size distributions (see Figure 3b and Figure A (supplementary material)) of the product suspension are found, i.e. obviously catastrophic fracture of the stressed non-brittle polymer particle leading to multiple smaller fragments is not the dominant size reduction mechanism, but size reduction occurs more likely by a shearing-off mechanism. For process times of more than 515 minutes the particle size distribution shifts to a monomodal distribution and, thus, becomes narrower again (Figure A, supplementary material). Moreover, only negligible changes in the product particle size $x_{50,3}$ have been observed and a limiting value of about 13 µm has been found under the chosen process conditions. Structural characterization of the comminution products by dynamic scanning calorimetry (see section 3.5.1) and infrared spectroscopy (supplementary information) has been performed for the samples collected after 60 minutes, 180 minutes, 240 minutes and 345 minutes (‘ground PBT’) obtained by a separate grinding experiment and represented by the cross symbols.

The behavior of wet-ground PBT powder in laser beam melting of polymers has been studied for the product ‘ground PBT’ of particle size $x_{50,3}$ = 25.2 µm. This sample has been obtained after wet grinding for approximately 5.5 hours and subsequent centrifugation and drying of the sediment. Plate-like primary particles are obtained (Figure B, supplementary material).

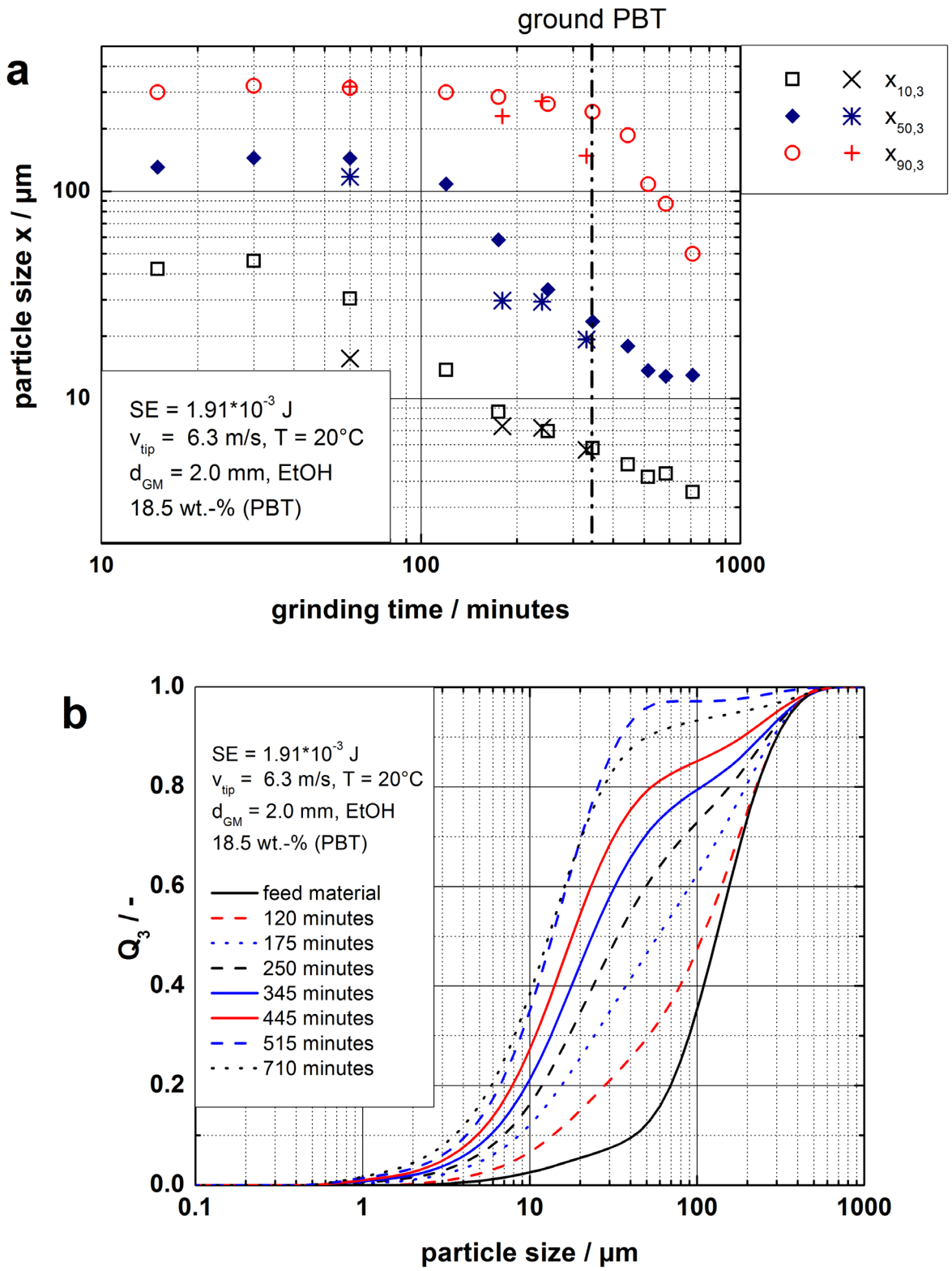

Figure 3: (a) Evolution of product particle sizes $x_{10,3}$, $x_{50,3}$ and $x_{90,3}$ during wet grinding of PBT in ethanol. (b) cumulative particle size distributions (Q_3, volume) of the product particles for different process times.

3.2 Rounding of PBT

For rounding the temperature profile given in Figure 2 (right) was applied and the residence time of the particles in the melting zone ($T_{Measured}$ > 230 °C) was set to 7.7 s by choosing a sheath gas flow of 4 m^3/h and an aerosol gas flow of 3 m^3/h. For calculation of the residence time laminar flow and no back-mixing of particles and gas (Brust and Wirth, 2004) in the reactor can be assumed. Ground PBT was used as feed material. Rounded PBT (c.f. Figures 1 and 4) with $x_{50,3}$ = 18.8 µm ($x_{10,3}$ = 8.2 µm, $x_{90,3}$ = 45.7 µm) was obtained for these process conditions. In the following the rounding process and especially the choice of proper process conditions is discussed. The residence time necessary for complete rounding can be calculated applying a viscous flow-sintering model (Kirchhof et al., 2009). As demonstrated for the rounding of polystyrene (Schmidt et al., 2014), characteristic sintering times obtained for three-dimensional particle aggregates (made up of primary particles of same size) using the viscous flow sintering model (Kirchhof et al., 2009) provide a reasonable estimate for the minimum residence time needed for (complete) rounding of the irregular-shaped comminution products. In the framework of the aforementioned model the Navier-Stokes equations are solved by a fractional volume of fluid method and particle-particle interactions are taken into account. The sintering time t necessary to obtain a single spherical particle from an aggregate of final radius a_f according to the model is given by equation 3. The structure of the initial aggregate does not affect the necessary sintering time needed to obtain a fully coalesced sphere (for details on this issue please refer to (Kirchhof et al., 2009; Schmidt et al., 2014)).

$$\text{(eq. 3)}\quad t = \frac{4.20 \cdot \eta \cdot a_f}{\sigma}$$

The main influencing parameters are the surface tension σ and the melt viscosity η of the polymer. Taking typical material parameters of PBT into account, i.e. a surface tension of the melt of σ = 30.2 mN/m (Ito et al., 2008) and a melt viscosity of η = 452 Pas (Fakirov, 2002), a characteristic sintering time of about 1.5 s is calculated for particles sized a_f = 0.5 * $x_{90,3}$ (rounded PBT) = 22.9 µm using equation 3, i.e. the residence time chosen (7.7 s) allows for complete rounding. Almost perfect spherical particles are obtained (see Figure 4a).

3.3 Dry particle coating of PBT

The rounded PBT already shows improved flowability and higher bulk density as compared to the ground PBT (see section 3.4). To further improve the flowability dry particle coating (Rumpf, 1974; Pfeffer et al., 2001; Yang et al., 2005) of the polymer microparticles using fumed silica was performed. By dry particle coating nanoscale silica (guest) particles are

attached due to van der Waals forces onto the surfaces of the PBT (host) microparticles. PBT-silica composite particles with surfaces showing nano roughness are obtained: The nanoscale particles act as ‘spacers’ between the host particles, i.e. they increase the interparticulate distance between two adjacent host particles which leads to a decrease of the (attractive) van der Waals forces between them (Zhou et al., 2003; Zhou and Peukert, 2008; Götzinger and Peukert, 2004). In consequence, the flowability of dry coated powders increases, which is advantageous for the powder deposition step in laser beam melting of polymers leading to dense devices of improved surface quality (Blümel et al., 2015). SEM images of the particles ‘PBT rounded & dry coated’ obtained after the dry coating process are shown in Figure 4: the polymer particles’ surfaces are homogeneously covered with nanoscale SiO_2 particles (Figure 4b).

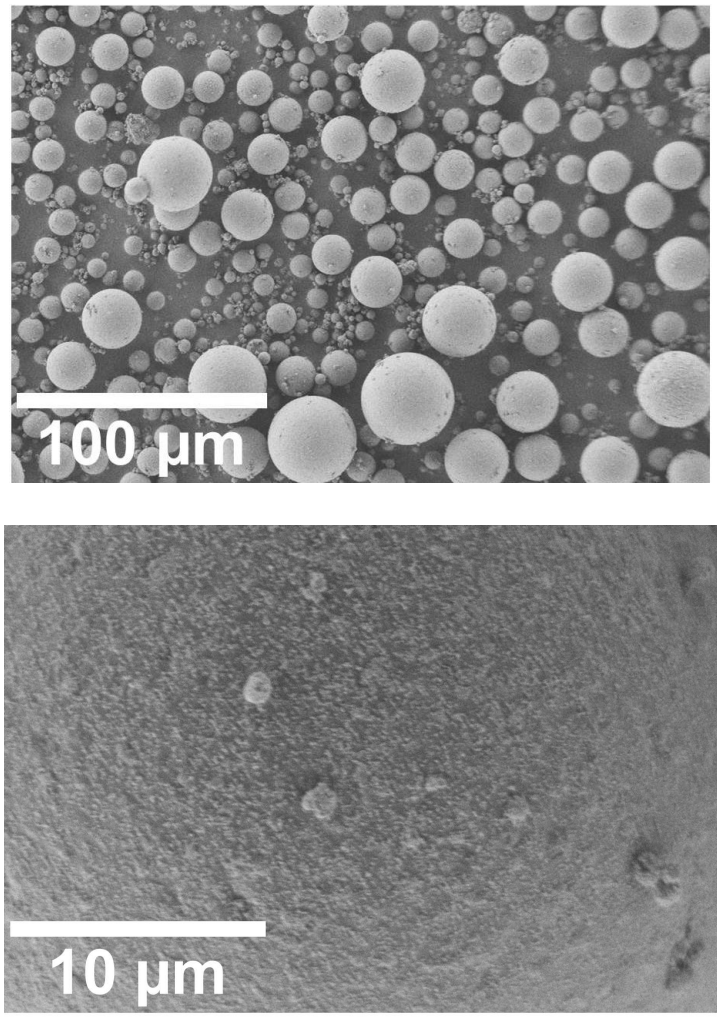

Figure 4: (a) SEM image of rounded & dry coated PBT obtained by dry coating of rounded PBT with fumed silica, (b) SEM image of the composite particle surface.

3.4 Bulk material properties and their implications on device quality

3.4.1 Tensile strength of powders and flowability

The effect of rounding and subsequent dry coating on the flowability of the powders has been studied using a tensile strength tester. In short, the device allows to assess interparticulate forces by measurement of the force needed to separate two adjacent layers of particles. For details on the procedure please refer to (Schweiger and Zimmermann, 1999; Meyer and Zimmermann, 2004; Schmidt et al., 2014). The measured tensile strength allows for predictions of powder flowability: with decreasing tensile strength the flowability increases. Moreover, the measurement is done for almost uncompacted powders, which is quite close to the conditions that apply for the powder deposition step in LBM. Besides tensile strength testing of powders and shear testers (Krantz et al., 2009; Blümel et al., 2015) a variety of alternative methods for the determination of quantities correlating with powder flowability have been proposed to characterize the flowability of powders used in additive manufacturing (Amado et al; Abdullah and Geldart, 1999; Freeman, 2007; Schmid, 2015): frequently the Hausner ratio, i.e. the ratio of tapped density and bulk density (Wudy and Drummer; Schmid, 2015) is used for prediction of powder flowability. Although good correlation between the Hausner ratio and flowability determined by shear testers has been reported in literature (Abdullah and Geldart, 1999; Saw et al., 2015) one should consider that the Hausner ratio strictly speaking is not a material property, because it depends amongst others on the consolidation procedure applied (c.f. number of taps, filling procedure) and may depend on the powder volume used and the geometry. To obtain comparable results standard protocols (see e.g. (Sousa e Silva, J P et al., 2013)) have to be followed. A similar situation holds true for the determination of flowability by funnels, the determination of the avalanche angle in rotating drums (Amado et al; Krantz et al., 2009), powder rheometers (Freeman, 2007) or the determination of the minimum fluidization velocity of a powder (Schmid, 2015; Ziegelmeier et al., 2015): Frequently remarkable good correlation of powder flowability as determined with shear testers and the results from the aforementioned characterization methods is found, however, in these empirical approaches the stress state of the powder frequently is not well defined and there may be influences of device geometry on the measured property, which thus is not a physical quantity in the classical meaning.

Tensile strengths of powders obtained after the single process steps are summarized in Table 1. As an estimate for the error of the tensile strength determined the standard deviation of three repetition measurements is reported. Moreover also data on bulk density as well as on solid density (determined by He pycnometry) are given in Table 1.

Table 1: Tensile strength, bulk density and solid density of the produced PBT powders.

	tensile strength / Pa	bulk density / g/cm^3	density / g/cm^3
PBT < 0.5 mm(feed)	n/a	n/a	1.30
ground PBT	15.7 +/- 0.8	0.25	1.32
rounded PBT	10.7 +/-1.7	0.47	1.34
rounded & dry coated)	2.9 +/- 0.6		

The PBT powder produced by wet grinding (ground PBT) shows a high tensile strength of around 16 Pa. It is cohesive and shows a rather poor flowability. Moreover, the irregular, plate-like particles (Figure B, supplementary material) show a low bulk density. Both, poor flowability and low bulk density are unfavorable in the LBM process: inhomogeneous powder deposition in the coating step will be a consequence of poor flowability. Powders of low bulk density, i.e. high porosity, do hardly consolidate during laser melting which will result in porous devices of poor dimensional accuracy. The rounding and the consecutive dry coating step improve the powder characteristics with respect to LBM processability: a remarkable increase of the bulk density of the powder obtained after rounding and a reduced tensile strength of approximately 11 Pa are found. Also a slight increase in solid density was observed. Dry coating results in a further decrease of the tensile strength of the powder (rounded & dry coated PBT) to about 3 Pa, which is comparable to commercially available PA12 materials used in LBM. Thus, an improvement of flowability by a factor of more than 5 is achieved by tailoring particle shape (rounding) and reducing the interparticle attractive forces by dry particle coating.

3.4.1 Powder deposition

Besides tensile strength measurements also a quantitative evaluation of powder deposition by doctor blading and image analysis was performed which gives the possibility to assess the processability of the powders during the application of a new powder layer in LBM. Figure 5 summarizes the powder deposition behavior. Three independent coating experiments were performed. Depending on the flowability of the respective powders only a certain area (white) is covered with particles after the deposition step: For ground PBT an area coverage of only (19.1 +/- 4.2) % was observed. The powder layer prepared from rounded PBT showed a coverage of (28.4 +/- 3.8) %. Remarkably, an almost complete surface coverage of (97.3 +/-

1.8) % is achieved for rounded & dry coated PBT. Small tensile strength of powders (good flowability) correlates with homogeneous powder deposition and almost complete surface area coverage.

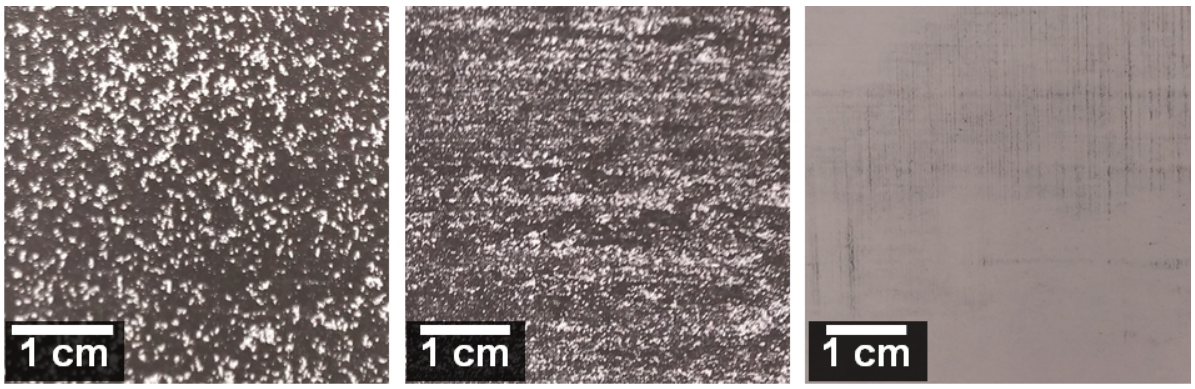

Figure 5: Powder deposition of ground PBT (left), rounded PBT (middle) and rounded & dry coated PBT (right) after doctor blading.

3.4.2 Topological characterization of thin layers

The influence of bulk material properties on device quality is reflected by photographs of thin layer specimen obtained for ground, rounded and rounded & dry coated PBT powder by laser beam melting of polymers shown in Figure 6. The correlation between particle shape, bulk density, flowability and quality of the built layers already is obvious: only porous, open structures are obtained if the LBM process is run with ground PBT. A remarkably improved layer quality is observed for specimens built from rounded powder: dense layers are obtained. The highest specimen quality is obtained from rounded & dry coated PBT: the devices appear smoother and show fewer defects. To quantify the thin layers' quality obtained from rounded and rounded & dry coated material, profilometry has been performed. A rms roughness R_{RMS} of (73.0 +/- 2.9) µm was found for the layer built from rounded powder, whereas a smaller roughness of R_{RMS} = (48.5 +/- 15.1) µm was determined for the specimen built from rounded & dry coated PBT. The errors given refer to the standard deviation of the determination of R_{RMS} for three different traces along the whole dimension of the specimen.

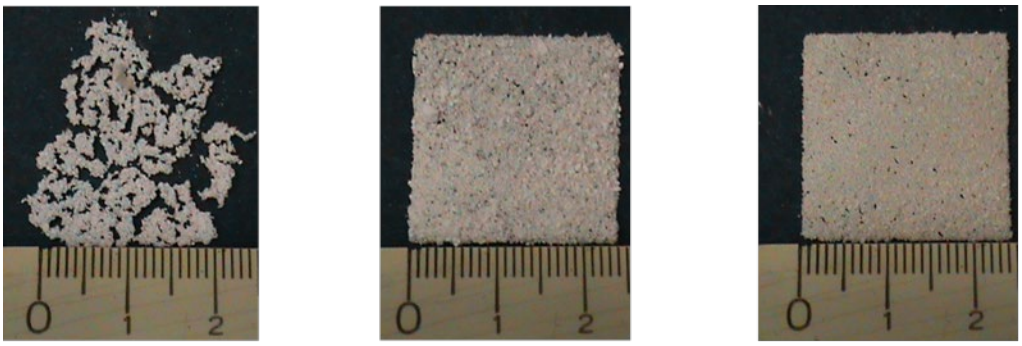

Figure 6: Thin layer specimen obtained by laser beam melting from (A) ground PBT, (B), rounded PBT and (C) rounded & dry coated PBT.

Also the characteristics of layers built via LBM directly correlate with the powder properties. Good flowability and high bulk density are a prerequisite for dense devices with a smooth surface.

3.5 Structural characterization of the powders along the process chain

Besides bulk material properties also the polymer structure will influence the LBM processability. Especially the degree of crystallinity is relevant for LBM processing. Structural changes of the material along the process chain have been monitored by dynamic scanning calorimetry, X-ray diffraction and infrared spectroscopy (see supplementary material). In this section the structural features of the particles and in the case of XRD also of the parts built from the respective powders are addressed.

3.5.1 Differential scanning calorimetry

Enthalpies of fusion ΔH_f and the melting temperatures T_{melt} of the PBT feed material, ground PBT, PBT comminution products withdrawn after shorter process times and rounded PBT, as determined by DSC, are summarized in Table 2. For a typical DSC curve, see Figure D in the supplementary information. Moreover, also the degree of crystallinity (α-PBT) calculated from the melting enthalpies of the processed powders, taking the melting enthalpy of fully crystalline α-PBT of ΔH_f^0 = 145.5 J/g (Vallejo et al., 2001) into account, are given.

Table 2: Melting temperature T_{melt}, enthalpy of fusion ΔH_f and degree of crystallinity (α-PBT) of different PBT materials ground and rounded, respectively, as determined by DSC.

	Melting temperature T_{melt} / °C	Enthalpy of fusion ΔH_f / J/g	Degree of crystallinity (α-PBT) / wt-%
feed material (PBT < 0.5 mm)	227.3	51.0	35.0
PBT, ground 60 minutes	226.4	49.8	34.3
PBT, ground 180 minutes	227.9	50.8	34.9
PBT, ground 240 minutes	228.4	52.8	36.3
ground PBT	228.4	52.5	36.1
rounded PBT	230.2	45.3	32.1 (*)

(*) sample contains also some β-PBT (c.f. section 3.5.2). The degree of crystallinity has been estimated assuming similar melting enthalpies for the α- and β-PBT polymorph.

No significant change of crystallinity during wet grinding is observed: an amount of 34.3 to 36.3 wt-% of α-PBT, corresponding to melting enthalpies between 49.8 J/g and 52.8 J/g, is found for the comminution products obtained for process times between 60 minutes and 330 minutes (c.f. ground PBT), which is the same crystallinity observed for the semi-crystalline PBT feed material (35.0 %) and quite common for commercial PBT grades. Therefore, we conclude that no amorphization of the semi-crystalline polymer occurs during comminution in the stirred media mill for the stressing conditions and process times considered. However, during the subsequent rounding step structural changes occur which are reflected in a change of thermochemical characteristics of the PBT powders: rounded PBT shows a smaller heat of fusion (45.3 J/g) than both, ground PBT and feed material. The reduced heat of fusion reflects a slightly lower degree of crystallinity. Moreover, in DSC an increased melting temperature of 230.2 °C is observed for the rounded material. An increase in melting temperature of PBT upon thermal annealing at temperatures above 205 °C, being due to structural changes (formation of different spherulitic structures), has been reported by Yeh and Runt (Yeh and Runt, 1989).

3.5.2 X-ray diffraction

Polybutylene terephthalate is known to exist as two polymorphs (α and β form) (Boye and Overton, 1974; Jakeways et al., 1975; Yokouchi et al., 1976). Both crystal modifications are triclinic. Transition from α-PBT to β-PBT is known to occur reversibly upon mechanical stressing: Yokouchi et al. (Yokouchi et al., 1976) obtained β-PBT from amorphous PBT after elongation of the amorphous polymer and subsequent heat treatment at 200 °C under tension. Upon relaxation they observed formation of α-PBT which could be transformed to β-PBT again upon stretching of about 12%. While in early work on the phase behaviour of PBT (Boye and Overton, 1974; Jakeways et al., 1975; Yokouchi et al., 1976) it was concluded that the β-polymorph only exists under tension, however more recent works (Roebuck et al., 1992; Carr et al., 1997) revealed that also a stable β phase can be observed, e.g. for spun and drawn PBT yarns (Carr et al., 1997). Moreover, formation of a stable β-PBT phase also has been reported for PBT blend systems (Tomar and Maiti, 2009). According to literature (Mencik, 1975; Yokouchi et al., 1976; Tomar and Maiti, 2009) the α and β phase of PBT can be discriminated by a reflex observed at 29.9° (Cu-K_α) only for β-PBT. X-ray diffraction pattern of the PBT feed as well as the obtained ground and rounded powders are depicted in Figure 7.

The XRD pattern of the feed material (PBT < 0.5 mm) and the PBT powder obtained after wet grinding (ground PBT) are almost the same. The patterns are typical for α-PBT and no remarkable changes of the structure due to grinding (c.f. no significant changes in absolute count rate or intensity ratios of different reflexes) occur. However, the XRD patterns observed for rounded PBT are different from the diffractogram of ground PBT: It is well-known that the crystallization behaviour of semi-crystalline thermoplasts is influenced by the temporal evolution of temperature, pressure and the stress state (c.f. shear vs. elongational stress). First, a new signal at 2Θ = 27.7 ° is observed which is assigned to the β-phase of PBT, i.e. the rounded PBT powder is a mixture of amorphous PBT (c.f. DSC characterization), α–PBT and β-PBT. Most probably, β-PBT is formed at the final stages of the rounding process, i.e. during the solidification of the spherical polymer melt droplets. As outlined above, β-PBT is known to be formed from amorphous and α-PBT upon elongation. Therefore, certain volume elements of the spherical particles formed during the rounding step in the downer reactor are subjected to tension built up by shrinkage of the polymer melt droplet during solidification. Moreover, the full width of half maximum of the peaks becomes smaller which might be due to the formation of larger crystallites during the rounding step and the subsequent solidification of the molten polymer. Also an increase in intensity of the peaks at 2Θ = 17.3 ° (010) and 2Θ = 25.2 ° (111) is observed.

The aforementioned structural changes are anticipated to be of minor importance with respect to the mechanical properties of the devices obtained by LBM because the device properties are determined by the degree of crystallinity than by the polymorph.

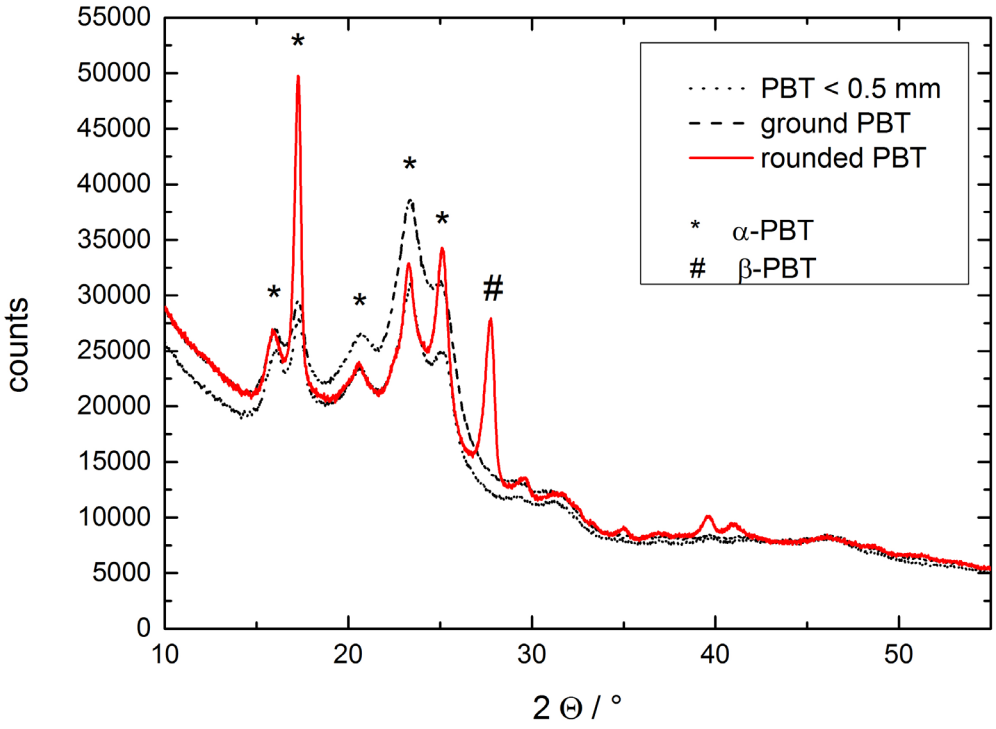

Figure 7: XRD patterns of PBT feed material (PBT < 0.5 mm) and powders obtained after wet grinding (ground PBT) and rounding (rounded PBT).

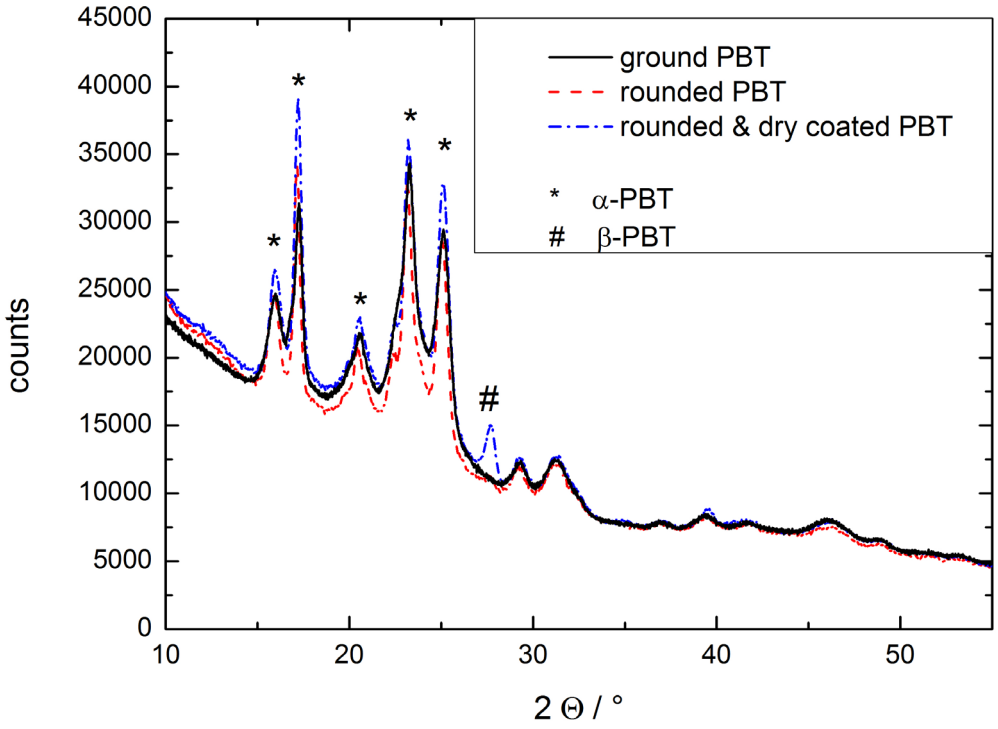

Figure 8: XRD pattern of thin layer devices built from ground PBT, rounded PBT and ground & rounded PBT.

The XRD patterns of thin layer devices built via LBM from different PBT powders are depicted in Figure 8. Thin layer devices built from ground PBT show a higher crystallinity as compared to the raw powder material due to melting and subsequent solidification (and partly crystallization) of the polymer powder during LBM processing. Besides amorphous material only the α-polymorph is found. In case of the rounded and the rounded and dry coated PBT powders, the devices obtained by LBM represent a mixture of amorphous PBT, α- and β-PBT similar to the raw powders. However, the relative amount of the β-polymorph (with respect to α-PBT) is somewhat lower in the devices, as compared to the respective powders, i.e. obviously relaxation of the structure takes at least place to a certain extent during LBM powder processing.

4. Conclusions

A process chain consisting of wet grinding, rounding in a heated downer reactor and dry coating has been applied to produce PBT powders of good flowability for laser beam melting of polymers. A thorough study on the structure of the polymer along the process chain as well as on the correlation between particle shape, tensile strength of the respective powders, bulk density and quality of thin layer specimens obtained via LBM has been performed.

The first step, wet comminution allows for tailoring the particle size without changing the crystallinity or structure of the PBT feed material as proven by DSC and XRD. A remarkable reduction of tensile strength of the powders is achieved by rounding. The change of the particle shape is accompanied by formation of some β-PBT which presumably is formed during the solidification of the polymer melt upon fast cooling. Dry coating, which is the third step, leads to a further decrease of powder tensile strength, i.e. improvement of powder flowability. An overall increase of flowability by a factor of 5 is accomplished by the change of the particle shape (rounding) and reduction of interparticulate van der Waals forces by dry coating of the particles.

The LBM processability of rounded and rounded & dry coated PBT powders has been demonstrated by thin layer specimens: For ground PBT powders only porous structures are obtained in LBM. The powders of improved flowability allow for dense parts of good surface quality. A correlation between particle shape, tensile strength of the respective powder, bulk density and thin layer quality has been demonstrated: Powders of good flowability and high bulk density are a prerequisite for parts of good quality. For rounded and dry coated PBT powder dense specimen of small rms roughness are obtained.

The process chain to produce spherical polymer powders of good flowability is versatile: all processes are scalable, i.e. the process chain can be transferred to the plant scale for production. Moreover, it may be applied to any polymer which may be comminuted and molten without degradation, i.e. it is applicable to a wide range of thermoplasts and therefore an option to widen the material spectrum of polymer powders for LBM.

Acknowledgements

German research foundation is acknowledged for funding of this study within the framework of CRC814 “Additive Manufacturing” (subprojects A1, A2, A3). The authors are grateful to Bettina Winzer (Institute of Particle Technology) for the support in tensile strength measurements and to Andreas Kunzmann (Institute of Physical Chemistry) for providing us access to the profilometry equipment.

Nomenclature

a_f	final particle radius (viscous flow sintering model= (Kirchhof et al., 2009)
d_f	focal diameter / m
d_{GM}	grinding media size / m

LBM	laser beam melting
P_l	laser power / W
PA	polyamide
PBT	polybutylene terephthalate
PEEK	poly ether ether ketone
Q_3	volume sum distribution / -
R_{RMS}	root mean square roughness
SE	stress energy / J
t	sintering time / s
$T_{Measured}$	measured temperature (downer reactor) / °C
T_{melt}	melting temperature / °C
T_{Set}	set temperature (heating of downer reactor) / °C
v_s	scan speed / m/s
v_{tip}	stirrer tip speed / m/s
x	particle size / m

Greek letters

ΔH_f	(mass-specific) heat of fusion / J/kg
η	viscosity / Pas
λ	wave length / m
ρ_{GM}	grinding media density / kg/m^3
σ	surface tension / N/m
θ	angle of diffraction / °

Literature

Abdullah, E.C., Geldart, D., 1999. The use of bulk density measurements as flowability indicators. Powder Technology 102 (2), 151–165.

Amado, A., Schmid, M., Levy, G., Wegener, K. Advances in SLS powder characterization. 22nd Annual International Solid Freeform Fabrication Symposium 2011, 438–452.

Bertling, J., Eloo, C., 2009. Verdichtetes Kohlendioxid als Prozessadditiv zur Herstellung polymerer und mikronisierter Nanokomposite: Schlussbericht "nanocrosser"; Förderzeitraum: 01.01.2006 - 31.12.2008.

Blümel, C., Sachs, M., Laumer, T., Winzer, B., Schmidt, J., Schmidt, M., Peukert, W., Wirth, K.-E., 2015. Increasing flowability and bulk density of PE-HD powders by a dry particle coating process and impact on LBM processes. Rapid Prototyping Journal 21 (6), 697–704.

Boye, C.A., Overton, J.R., 1974. Reversible, stress-induced, solid-phase transition in poly(tetramethylene terephthalate). Bulletin of the Amercian Physical Society 19 (3), 352.

Brust, H., Wirth, K.-E., 2004. Residence Time Behavior of Gas in a Downer Reactor. Ind. Eng. Chem. Res. 43 (18), 5796–5801.

Carr, P.L., Jakeways, R., Klein, J.L., Ward, I.M., 1997. Tensile drawing, morphology, and mechanical properties of poly(butylene terephthalate). J. Polym. Sci. B Polym. Phys 35 (15), 2465–2481.

Damm, C., Körner, J., Peukert, W., 2013. Delamination of hexagonal boron nitride in a stirred media mill. J Nanopart Res 15 (4).

Drexler, M., Drummer, D., Wudy, K., 2013. Effects of the powder bulk density on the porosity of laser molten thermoplastic parts. Proceedings of the Polymer Processing Society 29th Annual Meeting.

Drummer, D., Drexler, M., Wudy, K., 2015. Density of Laser Molten Polymer Parts as Function of Powder Coating Process during Additive Manufacturing. Procedia Engineering 102, 1908–1917.

Drummer, D., Rietzel, D., Kühnlein, F., 2010. Development of a characterization approach for the sintering behavior of new thermoplastics for selective laser sintering. Physics Procedia 5, 533–542..

Fakirov, S. (Ed.), 2002. Handbook of Thermoplastic Polyesters. Wiley-VCH Verlag GmbH & Co. KGaA, Weinheim, FRG.

Fanselow, S., Emamjomeh, S.E., Wirth, K.-E., Schmidt, J., Peukert, W., 2016. Production of spherical wax and polyolefin microparticles by melt emulsification for additive manufacturing. Chemical Engineering Science 141, 282–292.

Freeman, R., 2007. Measuring the flow properties of consolidated, conditioned and aerated powders — A comparative study using a powder rheometer and a rotational shear cell. Powder Technology 174 (1-2), 25–33.

Gibson, I., Shi, D., 1997. Material properties and fabrication parameters in selective laser sintering process. Rapid Prototyping Journal 3 (4), 129–136.

Goodridge, R.D., Tuck, C.J., Hague, R., 2012. Laser sintering of polyamides and other polymers. Progress in Materials Science 57 (2), 229–267. 10.1016/j.pmatsci.2011.04.001.

Götzinger, M., Peukert, W., 2004. Particle Adhesion Force Distributions on Rough Surfaces. Langmuir 20 (13), 5298–5303.

Ito, A., Konnerth, C., Schmidt, J., Peukert, W., 2016. Effect of polymer species and concentration on the production of mefenamic acid nanoparticles by media milling.

European journal of pharmaceutics and biopharmaceutics : official journal of Arbeitsgemeinschaft für Pharmazeutische Verfahrenstechnik e.V 98, 98–107.
Ito, E.N., Ueki, M.M., Bretas, R.E.S., Hage Junior, E., 2008. Interfacial tension of PBT/SAN blends by the drop retraction method. Mat. Res. 11 (2), 165–169.
Jakeways, R., Ward, I.M., Wilding, M.A., Hall, I.H., Desborough, I.J., Pass, M.G., 1975. Crystal deformation in aromatic polyesters. J. Polym. Sci. Polym. Phys. Ed 13 (4), 799–813.
Juhnke, M., Weichert, R., 2005. Zerkleinerung weicher Materialien ohne Verunreinigung der Produkte durch die Mahlkörper. Chemie Ingenieur Technik 77 (1-2), 90–94.
Kirchhof, M.J., Schmid, H.-J., Peukert, W., 2009. Three-dimensional simulation of viscous-flow agglomerate sintering. Physical review. E, Statistical, nonlinear, and soft matter physics 80 (2 Pt 2), 26319.
Krantz, M., Zhang, H., Zhu, J., 2009. Characterization of powder flow: Static and dynamic testing. Powder Technology 194 (3), 239–245.
Kruth, J.P., Wang, X., Laoui, T., Froyen, L., 2003. Lasers and materials in selective laser sintering. Assembly Automation 23 (4), 357–371.
Kwade, A., 1999. Determination of the most important grinding mechanism in stirred media mills by calculating stress intensity and stress number. Powder Technology 105 (1-3), 382–388.
Landwehr, D., Pahl, M.H., 1986. Kaltzerkleinerung von Gewürzen. Chemie Ingenieur Technik 58 (3), 246–247.
Linsenbühler, M., Wirth, K.-E., 2005. An innovative dry powder coating process in non-polar liquids producing tailor-made micro-particles. Powder Technology 158 (1-3), 3–20.
Mencik, Z., 1975. The crystal structure of poly(tetramethylene terephthalate). J. Polym. Sci. Polym. Phys. Ed 13 (11), 2173–2181.
Meyer, K., Zimmermann, I., 2004. Effect of glidants in binary powder mixtures. Powder Technology 139 (1), 40–54.
Nacken, T.J., Damm, C., Xing, H., Rüger, A., Peukert, W., 2015. Determination of quantitative structure-property and structure-process relationships for graphene production in water. Nano Res. 8 (6), 1865–1881.
Niedballa, S., 1999. Dispergierung von feinen Partikelfraktionen in Gasströmungen - Einfluss von Dispergierbeanspruchung und oberflächenmodifizierenden Zusätzen. Dissertation Technische Universität Bergakademie Freiberg, Freiberg.
Pfeffer, R., Dave, R.N., Wei, D., Ramlakhan, M., 2001. Synthesis of engineered particulates with tailored properties using dry particle coating. Powder Technology 117 (1-2), 40–67.
Roebuck, J., Jakeways, R., Ward, I., 1992. The existence of a stable β form in oriented poly(butylene terephthalate). Polymer 33 (2), 227–232.
Romeis, S., Hoppe, A., Eisermann, C., Schneider, N., Boccaccini, A.R., Schmidt, J., Peukert, W., Bose, S., 2014. Enhancing In Vitro Bioactivity of Melt-Derived 45S5 Bioglass ® by Comminution in a Stirred Media Mill. J. Am. Ceram. Soc. 97 (1), 150–156.
Rumpf, H., 1974. Die Wissenschaft des Agglomerierens. Chemie Ing. Techn. 46 (1), 1–11.
Saw, H.Y., Davies, C.E., Paterson, A.H., Jones, J.R., 2015. Correlation between Powder Flow Properties Measured by Shear Testing and Hausner Ratio. Procedia Engineering 102, 218–225.
Schäfer, M., Kemtchou, V.T., Peuker, U.A., 2016. The grinding of porous ion exchange particles. Powder Technology 291, 14–19.
Schmid, M., 2015. Selektives Lasersintern (SLS) mit Kunststoffen: Technologie, Prozesse und Werkstoffe. Hanser, München.

Schmidt, J., Plata, M., Tröger, S., Peukert, W., 2012. Production of polymer particles below 5µm by wet grinding. Powder Technology 228, 84–90.
Schmidt, J., Sachs, M., Blümel, C., Winzer, B., Toni, F., Wirth, K.-E., Peukert, W., 2014. A novel process route for the production of spherical LBM polymer powders with small size and good flowability. Powder Technology 261, 78–86.
Schweiger, A., Zimmermann, I., 1999. A new approach for the measurement of the tensile strength of powders. Powder Technology 101 (1), 7–15.
Sousa e Silva, J P, Splendor, D., Goncalves, I.M.B., Costa, P., Sousa Lobo, J.M., 2013. Note on the measurement of bulk density and tapped density of powders according to the European Pharmacopeia. AAPS PharmSciTech 14 (3), 1098–1100.
Tomar, N., Maiti, S.N., 2009. Thermal and crystallization properties of PBT/ABAS blends. J. Appl. Polym. Sci 113 (3), 1657–1663.
Vallejo, F.J., Eguiazàbal, J.I., Nazàbal, J., 2001. Solid state features and mechanical properties of PEI/PBT blends. J. Appl. Polym. Sci. 80 (6), 885–892.
Weber, A., Teipel, U., Nirschl, H., 2006. Comparison of Comminution by Impact of Particle Collectives and Other Grinding Processes. Chem. Eng. Technol. 29 (5), 642–648.
Wendel, B., Rietzel, D., Kühnlein, F., Feulner, R., Hülder, G., Schmachtenberg, E., 2008. Additive Processing of Polymers. Macromol. Mater. Eng. 293 (10), 799–809.
Wilczek, M., Bertling, J., Hintemann, D., 2004. Optimised technologies for cryogenic grinding. International Journal of Mineral Processing 74, S425-S434.
Witt, G., 2016. Neue Entwicklungen in der Additiven Fertigung. Springer Berlin Heidelberg.
Wohlers, T.T., 2014. Wohlers report 2014: 3D printing and additive manufacturing state of the industry annual worldwide progress report. Wohlers Associates, Fort Collins, Col.
Wolff, M., Antonyuk, S., Heinrich, S., Schneider, G.A., 2014. Attritor-milling of poly(amide imide) suspensions. Particuology 17, 92–96.
Wudy, K., Drummer, D. Aging behavior of polyamide 12 during selective laser melting process - influence on mechanical properties. SPE Proceedings ANTEC 2015, 2356–2363.
Yang, J., Sliva, A., Banerjee, A., Dave, R.N., Pfeffer, R., 2005. Dry particle coating for improving the flowability of cohesive powders. Powder Technology 158 (1-3), 21–33.
Yeh, J.T., Runt, J., 1989. Multiple melting in annealed poly(butlene terephthalate). J. Polym. Sci. B Polym. Phys. 27 (7), 1543–1550.
Yokouchi, M., Sakakibara, Y., Chatani, Y., Tadokoro, H., Tanaka, T., Yoda, K., 1976. Structures of Two Crystalline Forms of Poly(butylene terephthalate) and Reversible Transition between Them by Mechanical Deformation. Macromolecules 9 (2), 266–273.
Zhou, H., Götzinger, M., Peukert, W., 2003. The influence of particle charge and roughness on particle–substrate adhesion. Powder Technology 135-136, 82–91.
Zhou, H., Peukert, W., 2008. Modeling Adhesion Forces between Deformable Bodies by FEM and Hamaker Summation. Langmuir 24, 1459-1468.
Ziegelmeier, S., Christou, P., Wöllecke, F., Tuck, C., Goodridge, R., Hague, R., Krampe, E., Wintermantel, E., 2015. An experimental study into the effects of bulk and flow behaviour of laser sintering polymer powders on resulting part properties. Journal of Materials Processing Technology 215, 239–250.

Supplementary Material

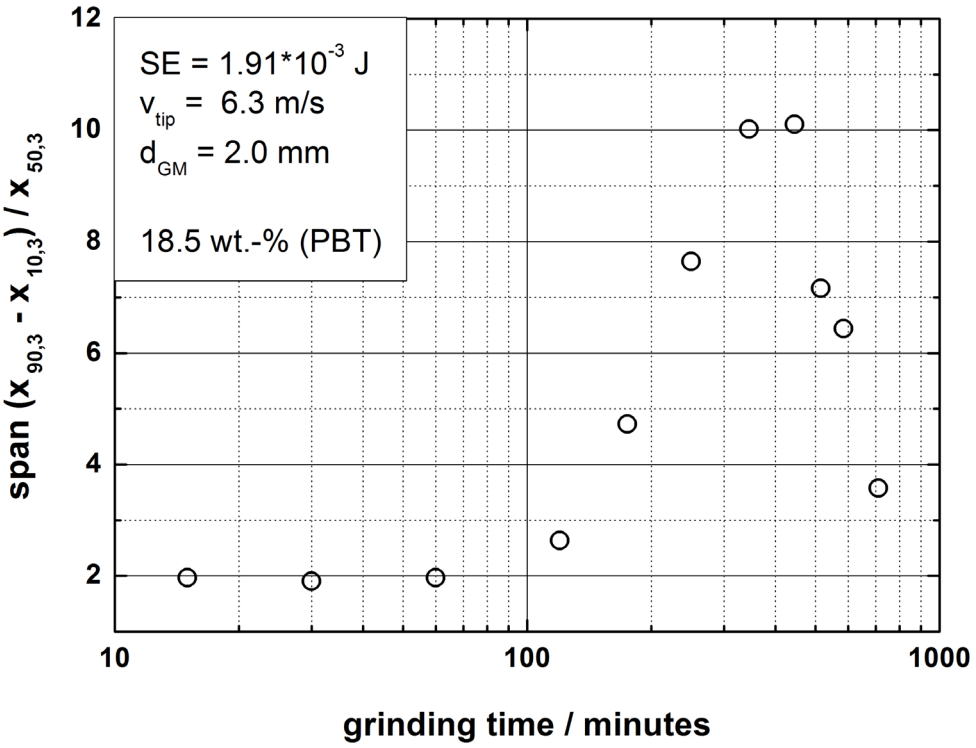

Figure A: Evolution of span ($x_{90,3} – x_{10,3}$) / $x_{50,3}$ over process time during wet grinding of PBT (stressing conditions: SE = 1.91 mJ, v_{tip} = 6.3 m/s, d_{GM} = 2.0 mm, feed concentration 18.5 wt-%, process temperature 20 °C).

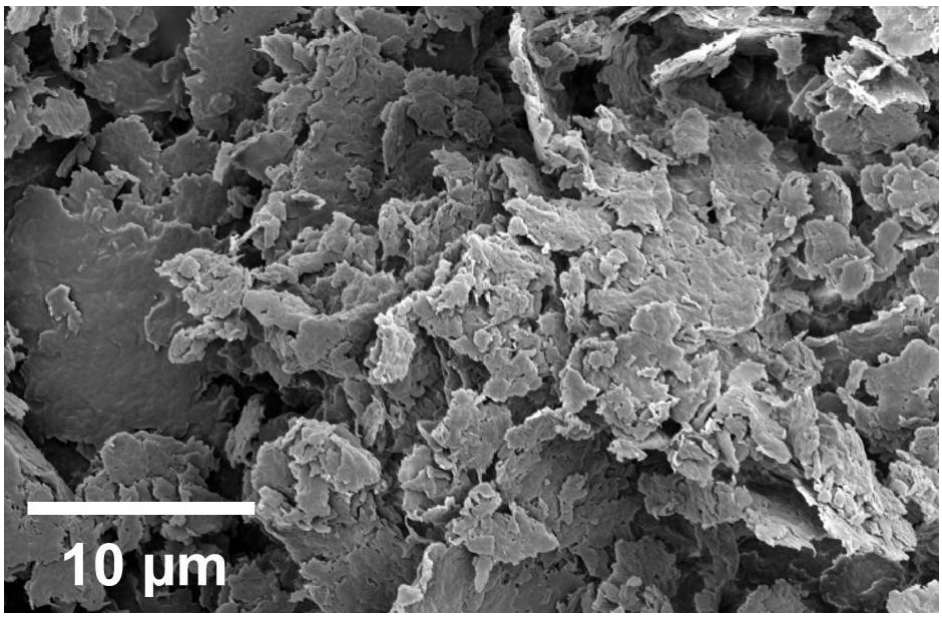

Figure B: SEM image of ground PBT obtained after about 5.5 hours of wet grinding (stressing conditions: SE = 1.91 mJ, v_{tip} = 6.3 m/s, d_{GM} = 2.0 mm, feed concentration 18.5 wt-%, solvent: ethanol, process temperature 20 °C).

Infrared spectroscopy

Infrared spectra of rounded PBT as well as PBT comminution products obtained for different process times are given in Figure C. For all samples spectral features being typical for PBT (Tomar and Maiti, 2009; Käppler et al., 2015) are found, i.e. the C=O vibrational band at around 1715 cm^{-1}, the CH_2 bending mode at 1503 cm^{-1} and the CH_2 wagging mode at 1530 cm^{-1} of the butylene units, the symmetric and asymmetric C-O-C stretching modes at 1206 cm^{-1} and 1103 cm^{-1}, respectively, as well as modes due to the aromatic ring at 1409 cm^{-1}, 1504 cm^{-1} and 1018 cm^{-1}, 873 cm^{-1} and 727 cm^{-1}. The spectra of the wet comminuted PBT powders are almost identical i.e. no pronounced changes in molecular structure during grinding of PBT for process times of up to 345 minutes at the stressing conditions summarized in section 3.1 occur. This indication corresponds well to the observations during DSC characterization of the respective powders.

Only minor changes are observed for rounded PBT: compared to the ground material a reduced intensity in the OH region (3700-3200 cm^{-1}) is observed, which might be due the removal of water from the material during rounding and subsequent solidification and (partial) crystallization. The change in crystallinity observed by DSC could not be detected by IR spectroscopy. It has been reported that amorphous PBT and the crystalline polymorphs may be discriminated in the spectral region of the methylene rocking (900-1000 cm^{-1}) and the methylene bending vibration (1300-1550 cm^{-1}). Stambaugh et al. (Stambaugh et al., 1979) assigned the bands at 917 cm^{-1} and at 1456 cm^{-1} to the unstressed alpha-phase whereas bands found at 935 cm^{-1} and 1388 cm^{-1} have components of both crystalline polymorphs. Amorphous PBT shows bands at 938 cm^{-1} and 960 cm^{-1}.

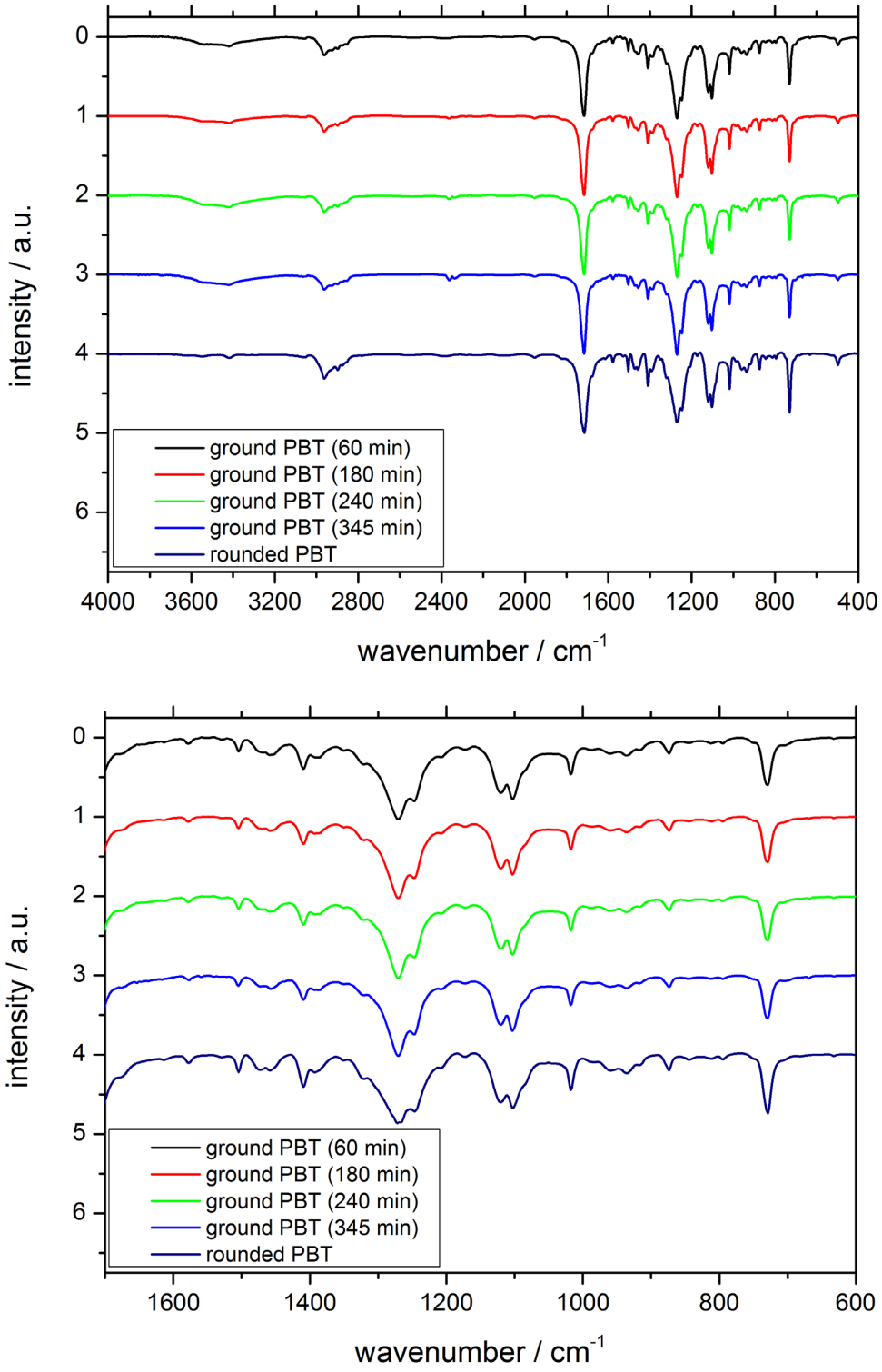

Figure C: IR spectra of wet comminuted PBT and rounded PBT powders in the wavenumber region (a) 4000 cm^{-1} to 400 cm^{-1} and (b) 1700 cm^{-1} to 600 cm^{-1}.

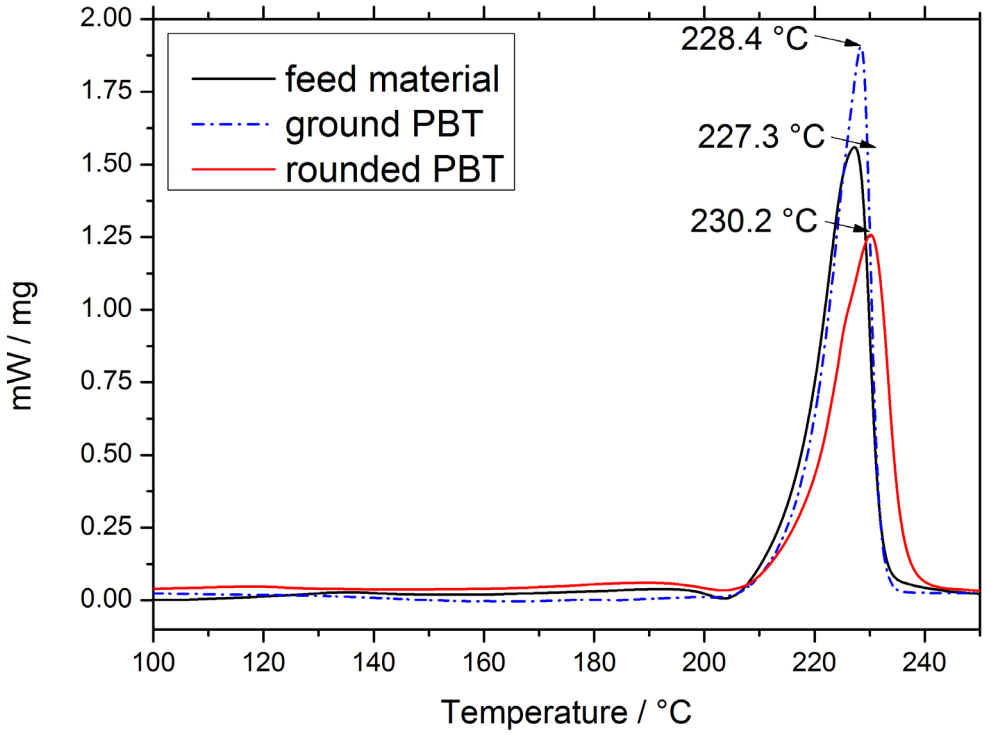

Figure D: DSC curves of PBT feed material, ground PBT and rounded PBT.

Literature

Käppler, A., Windrich, F., Löder, M., Malanin, M., Fischer, D., Labrenz, M., Eichhorn, K.-J., Voit, B., 2015. Identification of microplastics by FTIR and Raman microscopy: a novel silicon filter substrate opens the important spectral range below 1300 cm−1 for FTIR transmission measurements. Analytical and Bioanalytical Chemistry. 10.1007/s00216-015-8850-8.

Stambaugh, B., Lando, J.B., Koenig, J.L., 1979. Infrared studies of the reversible stress-induced crystal-crystal phase transition of poly(tetramethylene terephthalate). J. Polym. Sci. Polym. Phys. Ed. 17 (6), 1063–1071. 10.1002/pol.1979.180170614.

Tomar, N., Maiti, S.N., 2009. Thermal and crystallization properties of PBT/ABAS blends. J. Appl. Polym. Sci 113 (3), 1657–1663. 10.1002/app.30172.